UMYU Scientifica, Vol. 5 NO. 2, June 2026, Pp 336 – 352
https://doi.org/10.56919/usci.2652.031
ISSN: 2955 – 1145 (print); 2955 – 1153 (online)
A periodical of the Faculty of Natural and Applied Sciences, UMYU, Katsina

ORIGINAL RESEARCH ARTICLE

Mechanochemical Synthesis of a Biphenyl dicarboxylic acid-Based Zinc Metal Organic Framework for Brilliant Blue Dye Removal: Optimization by Box–Behnken Response Surface Methodology

Olaniran Kolawole Akeremale[1]*, Kamaluddeen Suleiman Kabo[2] and Ikechukwu Ogadimma Alisi[3]
[1]Department of Science and Technology Education, Bayero University, 3011, Kano, Nigeria
[2]Department of Chemistry, Federal University Dutsin-Ma, 5001, Katsina, Nigeria
[3]Department of Industrial Chemistry, Federal University Dutsin-Ma, 5001, Katsina, Nigeria

ABSTRACT

In this research, the optimization of Brilliant Blue dye (BBD) removal from aqueous solution was investigated using a zinc-based metal-organic framework (Zn-MOF) synthesized from 4,4-biphenyl dicarboxylic acid (BPDC) via a solvent-free mechanochemical approach using a mortar and pestle. The prepared adsorbent was characterized using Fourier Transform Infrared Spectroscopy (FTIR), Energy Dispersive X-ray Fluorescence (EDXRF), Brunauer–Emmett–Teller (BET) analysis, X-ray Diffraction analysis (XRD), Thermogravimetric Analysis (TGA) and pH point of zero charge (pH_{PZC}) measurements to evaluate its structural features, elemental composition, surface properties, thermal stability and surface charge behavior. The BET surface area was 221.022 m²/g, the pHPZC was 6, and the material was stable up to 310 °C. Statistical optimization of the adsorption process was carried out using Response Surface Methodology based on the Box–Behnken design. The effects of pH, ionic strength, contact time, and adsorbent dosage were examined as independent process variables, while percentage dye removal served as the response. In this study, the initial dye concentration was set at 30 Mg/L, the Sorbate volume was 100 mL, and dye concentrations were determined using a Jenway 7315 spectrophotometer at 640 nm, as obtained from the spectra scan of the dye. The optimized conditions obtained were an adsorbent dosage of 0.473 g, an ionic strength of 0.0017 mol/L, a contact time of 34.66 min, and a pH of 2.12. Under these conditions, an experimental dye removal efficiency of 98.33% was achieved, which was in close agreement with the model-predicted value of 99.16%, indicating the suitability of the model for the optimization of Brilliant Blue dye adsorption in a synthetic wastewater system.

ARTICLE HISTORY

Received March 24, 2026
Accepted June 26, 2026
Published June 39, 2026

KEYWORDS

Adsorption, BPDC linker, Mechanochemical Synthesis, Brilliant Blue Dye, RSM-BBD, Wastewater Treatment, Zn-MOF

INTRODUCTION

One of the biggest issues facing human society today is the scarcity of clean water; therefore, removing harmful and harmless contaminants from water resources has become crucial (Selvam *et al.,* 2008; Olaseni *et al.,* 2019). Artificial dyes and colourants are major sources of water pollution; they don't just alter the transparency of water systems but also introduce health hazards to humans, either directly or indirectly (Yu *et al.,* 2019; Akeremale and Olaseni, 2019). It is known that more than 100,000 commercial dyes are produced and discharged into our water bodies each year without any purification (Tkaczyk *et al.,* 2020). These highly water-soluble effluents are unwanted in our environment, as they are carcinogenic to both humans and animals and toxic to aquatic life (Imran *et al.,* 2021).

Brilliant Blue dye (BBD) is an aqueous triphenylmethane synthetic dye that is widely used as an anionic blue dye in textile, food, pharmaceutical, and analytical industries, with a molecular formula of $C_{37}H_{34}N_2Na_2O_9S_3$, a molar mass of approximately 792.8 g/mol, and usually has a maximum absorption wavelength (λ_{max}) between 620–640 nm in aqueous solutions. (Alam *et al.,* 2024). BBD are known to be highly chemically stable and resists biodegradation, leading to their persistence in aquatic systems (Katheresan *et al.,* 2023). Numerous studies also report that prolonged exposure to BBD may result in cytotoxic and genotoxic effects, and that its presence in water systems reduces light penetration and disrupts aquatic ecosystems (Khan *et al.,* 2024; Mahmood *et al.,* 2024).

A wide range of physical and chemical techniques have been utilized and studied for the removal of dyes from aqueous solutions in wastewater before discharge into water bodies (Adamu & Salisu, 2024; Adeleke et al., 2025;

Correspondence: Olaniran Kolawole Akeremale. Department of Science and Technology Education, Bayero University, 3011, Kano, Nigeria. ✉ okakeremale.ste@buk.edu.ng.
How to cite: Akeremale, O. K., Kabo, K. S., & Alisi, I. O. (2026). Mechanochemical Synthesis of a Biphenyl dicarboxylic acid-Based Zinc Metal Organic Framework for Brilliant Blue Dye Removal: Optimization by Box–Behnken Response Surface Methodology. *UMYU Scientifica*, 5(2), 336 – 352. https://doi.org/10.56919/usci.2652.031

Habibu et al., 2023; Ibrahim et al., 2023). These include but not limited to electrolysis, flocculation, chemical oxidation, catalysis, biological degradation, and adsorption (Nidheesh *et al.,* 2023). Because of its ease of application, cost efficiency, safety, and non-generation of toxic products or sludge, adsorption has been the most widely used method for the removal of colourants from wastewater (Jawad *et al.,* 2023).

Several adsorbent materials have been investigated for the treatment of dye-contaminated wastewater, including bioadsorbents, metal oxides, polymers, and activated carbon (Ali *et al.,* 2022). Bioadsorbents such as algae, fungi, rice husks, and wheat straw are attractive due to their low cost and natural abundance availability, however, they often exhibit lower adsorption capacities and may require modification or pre-treatment to enhance their performance, thereby increasing overall treatment costs (Sari and Tuzen, 2008). Metal oxide nanoparticles, including iron oxide, titanium oxide, and zinc oxide, have also been explored because of their high surface area and abundance of active sites. Nevertheless, their tendency to aggregate, high production costs, and potential toxicity arising from metal ion release remain significant limitations (Liao et al., 2017; Ghosh and Gupta, 2013). Synthetic polymers such as polyacrylamide and polystyrene have demonstrated good adsorption performance and ease of functionalization, but concerns regarding their non-biodegradability, cost, and dye-dependent adsorption behaviour restrict their wider application (Pavan et al., 2014). The U.S. Environmental Protection Agency recognizes activated carbon as one of the most effective technologies for coloured wastewater treatment; however, its large-scale application is often constrained by high production and regeneration costs as well as rapid exhaustion of adsorption sites during continuous use (Xing et al., 2010). Consequently, increasing attention has been directed towards the development of alternative functional materials, including nanomaterials, porous materials, polymeric materials, and biomaterials, that combine high adsorption efficiency with economic and environmental sustainability for dye removal applications (Khan et al., 2020; Kalia et al., 2023).

Metal-Organic Frameworks (MOFs) are highly porous crystalline materials prepared by combining organic molecules with metal ions and carbon atoms. MOFs have received intense attention in recent years for applications across many scientific and technological fields (Duan *et al.,* 2023). Due to their relatively large surface areas, tunable pore sizes, and multiple functionalities, which are significant parameters in adsorption studies, MOF materials are of interest as adsorbents for the removal of dyes from aqueous media (Qiu *et al.,* 2022). Using the conventional route for the synthesis of these MOFS usually involves the use of large amounts of organic solvents, extreme temperatures, high energy consumption, and lengthy reaction periods. These conditions often raise production costs and have a negative effect on the environment (Akeremale, 2022; Akeremale *et al.,* 2025). Mechanochemical synthesis, on the other hand, offers greater environmental safety than the conventional method while still producing highly crystalline materials. This technique involves solvent-free grinding of the Ligand and metal ions with a grinding material, such as a mortar and pestle, to create MOFs in a limited time, with reduced power consumption (Akeremale *et al.*, 2023).

There are different techniques for optimizing processes, and Response surface methodology (RSM) is one that has prospered over time. This method enhances the overall efficiency of the process, leading to lower operational cost and faster experiments (Montgomery, 2020). RSM is an experimental design methodology that uses statistical and mathematical methods to model the experiment, assess the impact of specific parameters, and determine the optimal conditions for an optimal response with the fewest experimental runs. It uses one or more response to show the significance of different independent factors. By adjusting the design elements, the RSM approach seeks to obtain a favorable response and identify response variation in a specific direction (Lamidi *et al.,* 2022; Zaid *et al.,* 2022)

The novelty of this work lies in the mechanochemical synthesis of a Zn–BPDC MOF using a simple, sustainable mortar-and-pestle approach and its application for Brilliant Blue dye removal. The adsorption process was also optimized using the Box–Behnken response surface methodology to determine the optimal operating conditions. To the best of our knowledge, no previous study has reported this combination of mechanochemical Zn–BPDC MOF synthesis and RSM-based optimization for Brilliant Blue dye removal. The effect of process variables such as adsorbent dosage, contact time, ionic strength and pH of the solution was examined by response surface methodology (Box-Behnken design) (RSM-BBD; 3 levels and 4 factors). It was hypothesized that the mechanochemically synthesized Zn–BPDC MOF would effectively remove Brilliant Blue dye from aqueous solution, and that response surface methodology would provide a reliable means of identifying the individual and interactive effects of the operating variables and determining the optimum removal conditions. The objectives of this study are to synthesize a Zn–BPDC MOF via a mechanochemical route, evaluate its efficiency for the removal of Brilliant Blue from aqueous solution, and optimize the adsorption process using Box–Behnken response surface methodology. The effects of pH, adsorbent dosage, ionic strength, and contact time on dye removal efficiency were investigated, and optimum operating conditions were determined using the developed statistical model.

MATERIALS AND METHODS

Materials

All of the reactions were ground using an agate mortar and pestle. Sigma-Aldrich in the UK and Nanjing Forever Pharmacy Co., Ltd. in China provided the chemicals used in this experiment (HCl, NaOH, NaCl, Brilliant Blue dye (BBD), 4,4'-biphenyldicarboxylic acid (BPDC), ZnCl2, and KNO3) with purities greater than 99%. Without any additional purification, the components were utilized exactly as they were. Each solvent was analytically pure and used precisely as specified. The investigation's solvent was double-distilled water.

Preparation of the BPDC-based Zn-MOF

The Zn-BPDC MOF was synthesized through a solvent-free mechanochemical method using a 2:1 molar ratio of $ZnCl_2$ to 4,4'-BPDC. The use of excess zinc salt was intended to promote effective framework formation, minimize the presence of unreacted ligand molecules, and ensure complete coordination between the zinc ions and the carboxylate groups of the ligand. Similar metal-rich ratios have previously been reported for mechanochemically synthesized zinc-based MOFs, such as MOF-74 and Zn-pyrazine systems, in which enhanced coordination and framework formation were observed (Julien *et al.,* 2016). For the synthesis, 25 mmol (6.06 g) of 4,4'-BPDC and 50 mmol (6.815 g) of zinc chloride were ground manually in an agate mortar and pestle for 20 minutes until a crystalline powder was obtained (Głowniak *et al.,* 2024). Following synthesis, the material was purified by stirring it in ethanol inside a 100 mL beaker for 2 hours. The resulting mixture was then filtered, and the supernatant was discarded. This washing step was performed to remove residual salts, unreacted precursors, and loosely bound ligand molecules, thereby improving the material's purity, crystallinity, and pore characteristics. Finally, the synthesized MOF was activated by oven-drying at 50 °C for 24 hours before further use (Głowniak et al., 2024).

Characterization of Adsorbent (Zn-BPDC MOF)

The adsorption behaviour of the Zn-BPDC MOF adsorbent was investigated using a Jenway 7315 spectrophotometer. The infrared spectra of the adsorbent were recorded using an Agilent Technology Scientific FTIR spectrophotometer. The synthesized Zn–MOF sample's specific surface area, pore volume, and pore-size distribution were measured using nitrogen adsorption–desorption analysis. A Xenemetrix Energy-Dispersive X-ray Fluorescence (EDXRF) spectrometer with an X-ray tube operating at 40 kV and 6.6 mA (400 W) was used for elemental analysis. The device uses a high-resolution silicon drift detector (SDD) to precisely detect characteristic X-ray lines, with a rhodium anode as the X-ray source. The analysis was conducted using the Quantachrome NOVA Station, a surface area and pore analyzer (Quantachrome Instruments, USA). The adsorbent's point of zero charge (pH_{PZC}) was also determined to better understand the adsorption mechanism. The solid-addition method, as outlined by Balistrieri and Murray (1981), was used to assess this.

Adsorption Experiments Optimization for BBD Removal by Response Surface Methodology (Box-Behnken Design) (RSM-BBD)

A statistical and mathematical method called the Response Surface Methodology (RSM) is used to develop, improve, and optimize various processes, including adsorption studies (Hasanzadeh *et al.,* 2021). Using the input parameters, ANOVA (Analysis of Variance) builds a regression model to estimate the output variables (Chen *et al.,* 2022). Using the Design-Expert program (Version 13), a total of 29 experimental runs were generated, using the method described by Jang et al. (2020) to set percentage removal (% removal) as the response variable (Y) for the various process parameters considered. The studies were carried out in batches to examine the Zn-BPDC MOF's adsorption characteristics towards BBD. RSM-BBD was used to estimate the optimal concentration for each variable to remove BBD from solution. We also investigated the linear, quadratic, and interaction effects of the selected process variables on the removal of BBD. The independent parameters studied in this work include; adsorbent dosage (grams, X_1 or A), ionic strength (Mol/L, X_2 or B), contact time (minutes, X_3 or C), and pH (X_4 or D). Three levels (-1, 0, 1) was selected to be tested for each of the parameters, and their specific details include (Table 1): adsorbent dosage set at 0.1, 0.3, and 0.5 g; ionic strength at 0, 0.085, and 0.17 Mol/L; contact time at 30, 75, and 120 minutes; and pH at 2, 7, and 12. The quadratic equation below explained the System's response:

$$Y = \beta_0 + \Sigma\beta_i X_i + \Sigma\beta_{ii} X_{ii} + \Sigma\beta_{ij} X_i X_j + \varepsilon$$

Y represents the response variable in this model, which corresponds to the percentage of dye removal. The symbols *i* and *j* denote the index values used in the model. The term β_0 refers to the constant or intercept of the equation, while X_1, X_2, …, X_k represent the coded independent variables. The coefficient β_i accounts for the linear effect of each factor, β_{ii} for the quadratic (squared) effect, and β_{ij} for the interaction between variables. The error term ε reflects random variation in the system and accounts for the difference between the predicted and the experimental data (Hosseinpour *et al.,* 2011). Using 100 mL Erlenmeyer flasks filled with the adsorbate solutions and a shaker set to 160 rpm for each designated period (min^{-1}), each experimental run was conducted. A pH meter and 0.5 M NaOH/HCl were used to adjust the mixture's pH. The residual dye concentrations before and after treatment were determined by measuring the absorbance of the filtered solution at the maximum wavelength (λmax) of 640 nm using a Jenway 7315 spectrophotometer. The adsorption investigation was conducted under different conditions for each run, and levels of adsorption (q_t) at time t (mg/g) were estimate using the formula;

$$q_t = (C_0 - C_t)\, V/(W) \quad (1)$$

W stands for adsorbent mass (g), V for solution volume (L), C_t (mg/L) for dye concentration at any time t, and C_0 (mg/L) for initial dye concentration in this equation (Vinothkumar *et al.,* 2025).

The equilibrium adsorption capacity, q_e (mg/g), was calculated using these parameters and the subsequent equation:

$$q_e = (C_0 - C_e)V/(W) \quad (2)$$

where C_0 (mg/L) represents the initial dye concentration and C_e (mg/L) represents the equilibrium dye concentration. The % reduction of BBD was then calculated using the following calculation (Akeremale *et al.*, 2019):

$$\text{Removal efficiency (\%)} = (C_0 - C_e)/(C_0) \times 100 \quad (3)$$

Table 1. Independent process variables and their corresponding levels used in the RSM-BBD model (Yadav *et al.*, 2021)

Code	variable	Levels		
		—1	0	+1
A	Adsorbent dosage (g)	0.1	0.3	0.5
B	Ionic Strength (Mol/L)	0	0.085	0.17
C	Time (Min)	30	75	120
D	pH	2	7	12

Safety and Waste Management

All experimental procedures were conducted in accordance with standard laboratory safety protocols. Appropriate personal protective equipment, including laboratory coats, gloves, and safety glasses, was used throughout the study. Dye-containing solutions and chemical waste generated during the experiments were collected and disposed of in accordance with the host institution's waste management guidelines and applicable environmental regulations.

3. Results and Discussion

3.1 Results of synthesis and activation of the Zn-BPDC MOF

In order to obtain a crystalline Zn-BPDC-MOF, 6.06g (25 mmol) of the ligand and 6.82g (50 mmol) of the metal salt were weighed and ground for 20 minutes using an agate mortar and pestle. The resulting crystalline powder was then dissolved in ethanol, stirred for 2 hours, and filtered to remove unbound or unreacted precursor metal and chlorine atoms. After that, the material was dried in an oven at 50 °C for 24 hours to activate it. After washing and activation (drying), 9.46g of the synthesized compound was recovered from a total mass of around 12.88g of the ligand and metal salt. This indicates that 3.48g was lost during the washing stage, and the synthetic process produced a yield of almost 73.45%.

3.2 Characterization of the BPDC-based Zn-MOF adsorbent

The functional groups on the adsorbent surface were identified by Fourier transform infrared (FT-IR) spectroscopy (Figure 1) (Flórez *et al.*, 2024).

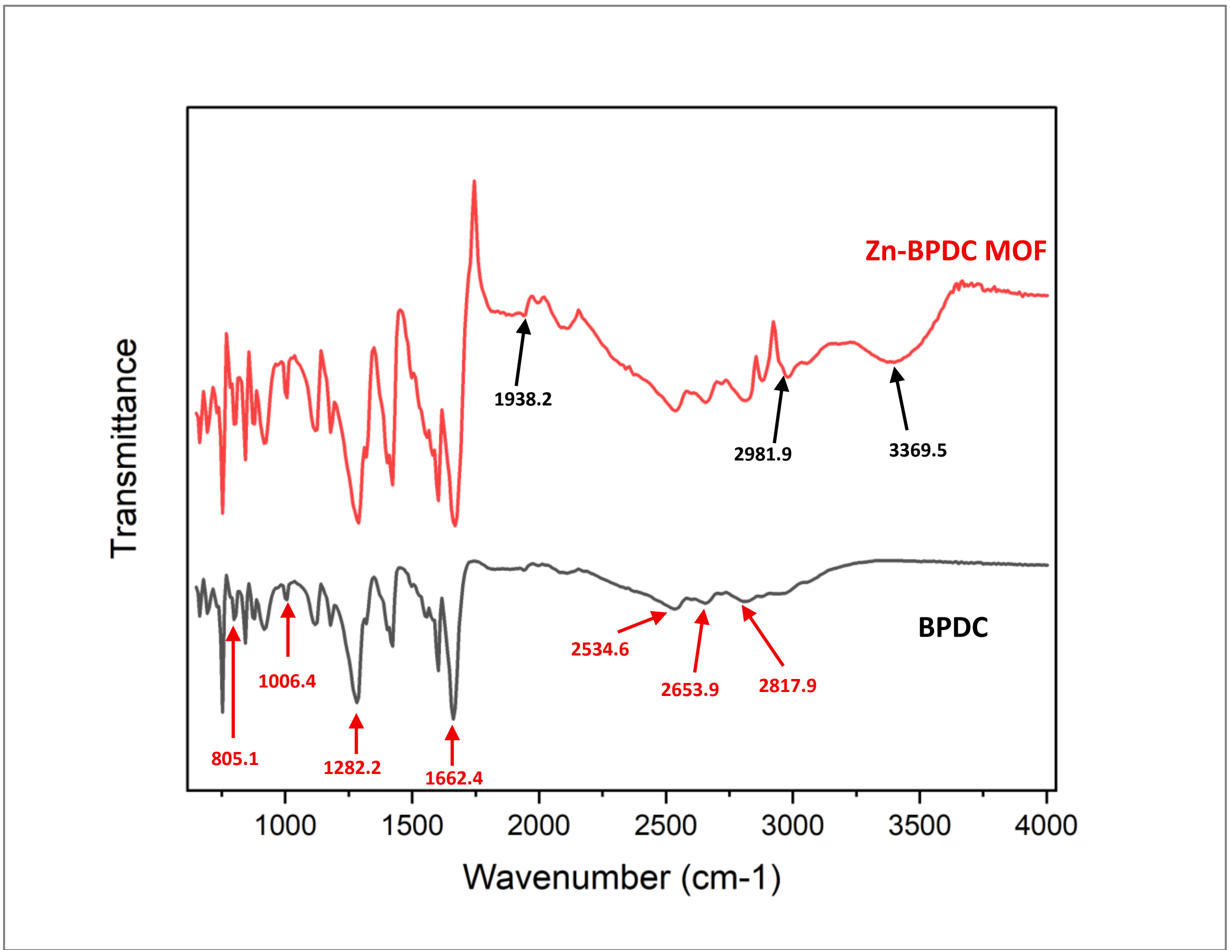

Figure 1: Zn-BPDC MOF and BPDC FT-IR Spectra.

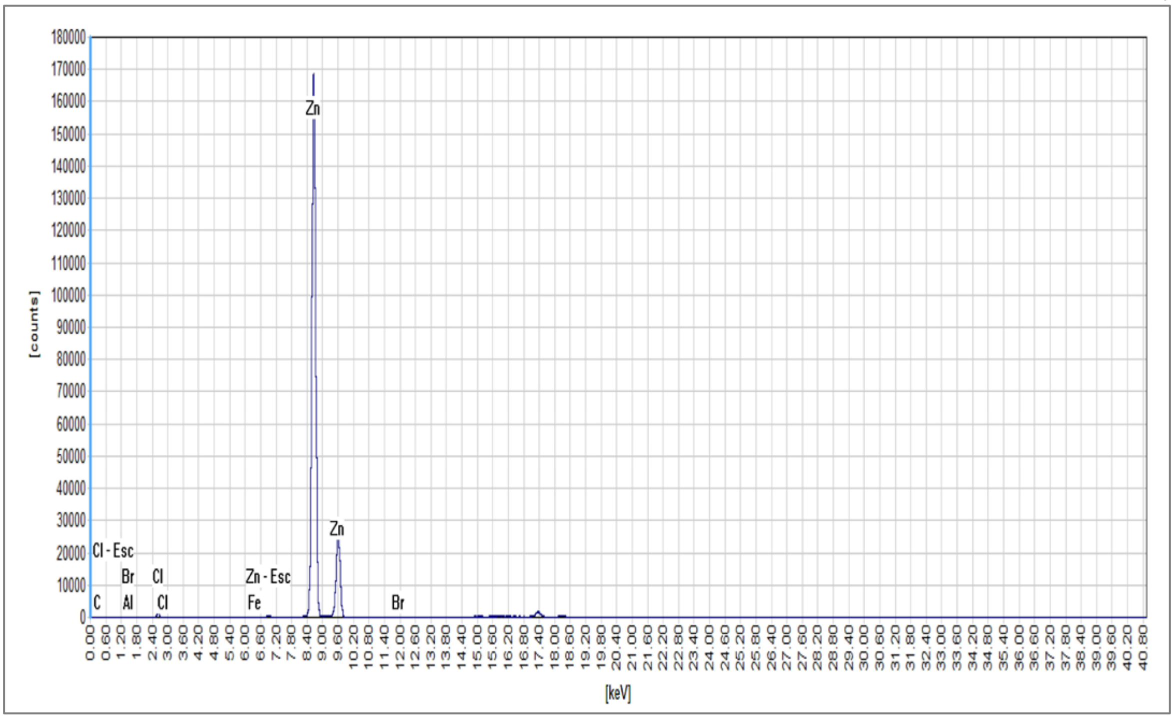

Figure 2: EDXRF spectra of Zn-BPDC MOF

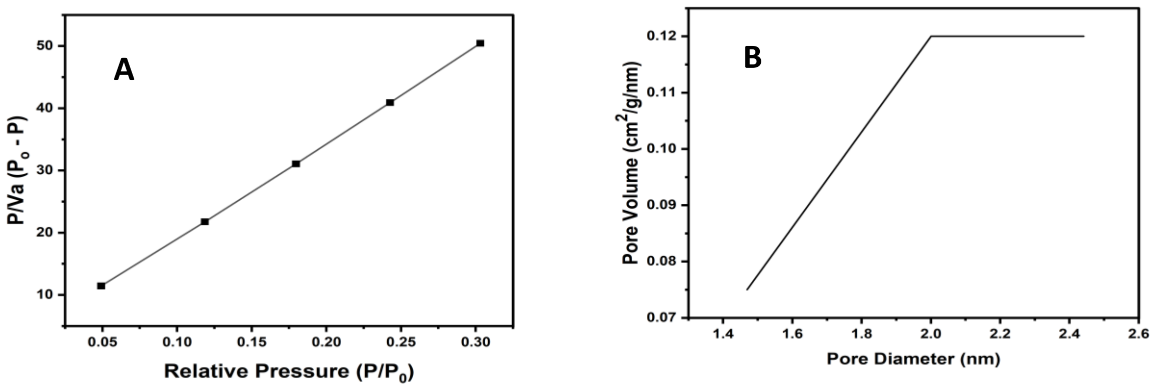

Figure 3: (A) Linear fitting Plot of Zn-BPDC MOF, (B) Pore volume plot of Zn-BPDC MOF

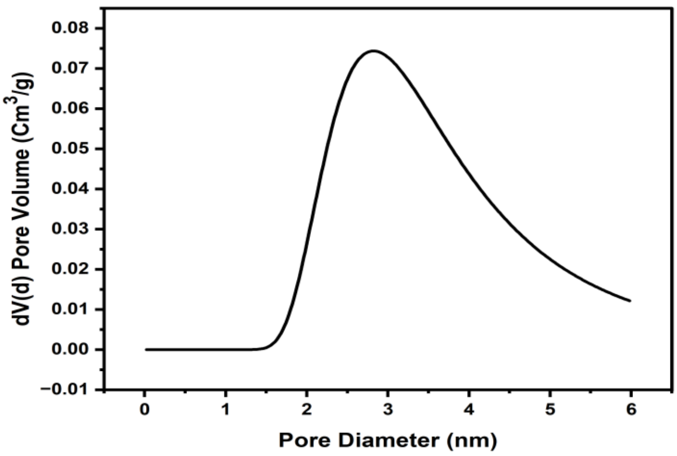

Figure 4: Pore size distribution plot

The BPDC ligand exhibits characteristic aromatic vibrations, which are compatible with biphenyl skeletal vibrations. These include para-disubstituted benzene C–H out-of-plane bending at 805 cm⁻¹ and additional aromatic ring deformation bands around 924 and 1006 cm⁻¹ (Smith, 2016). While the strong absorption at 1662 cm⁻¹ corresponds to C=O stretching of the carboxyl group, shifted to a lower wavenumber due to conjugation with the aromatic ring and solid-state interactions, the bands that appear in the 1100–1300 cm⁻¹ region are attributed to C–O stretching of carboxylic acid groups (Nandiyanto *et al.,* 2022).

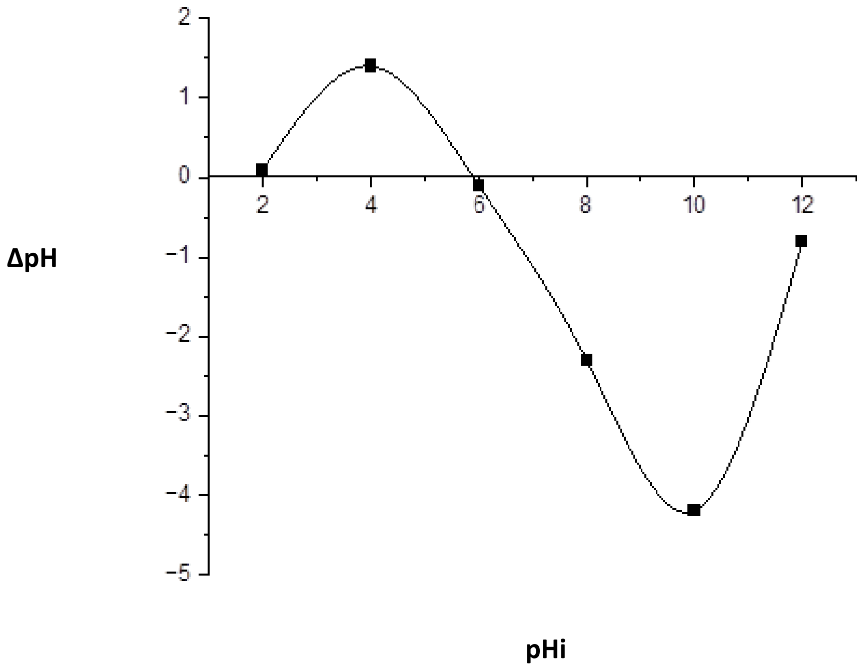

Figure 5: Plot of determination of pH_{PZC} of Zn−BPDC MOF

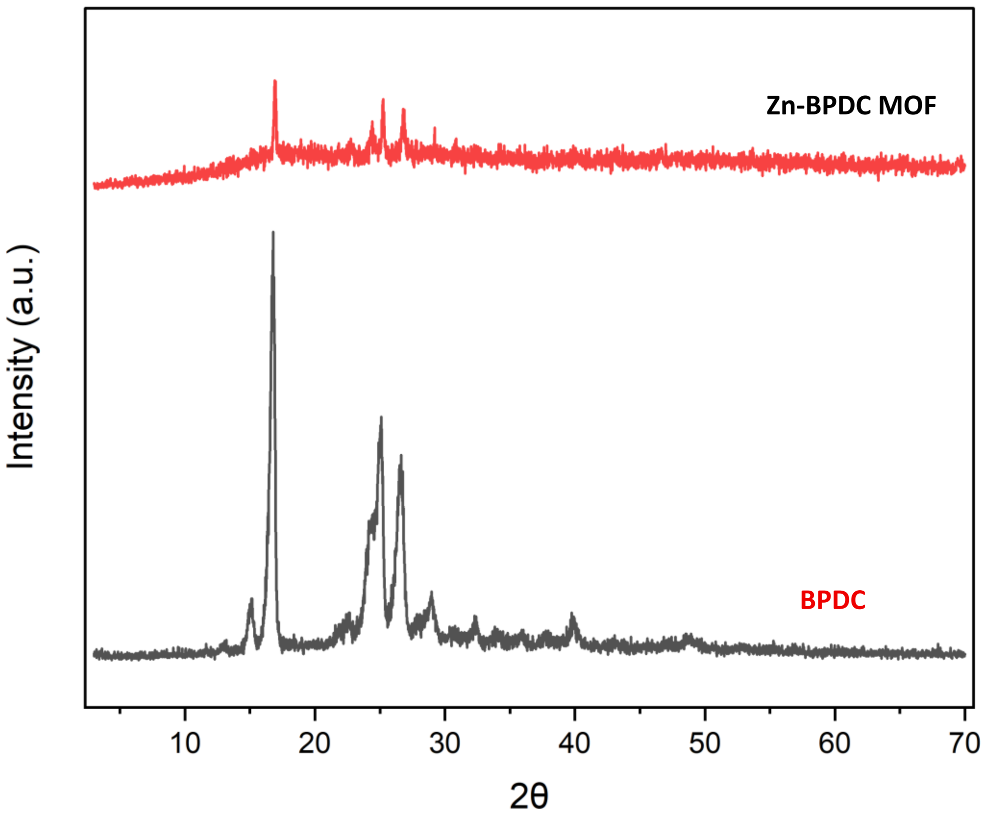

Figure 6: XRD patterns of pure BPDC and Zn-BPDC MOF

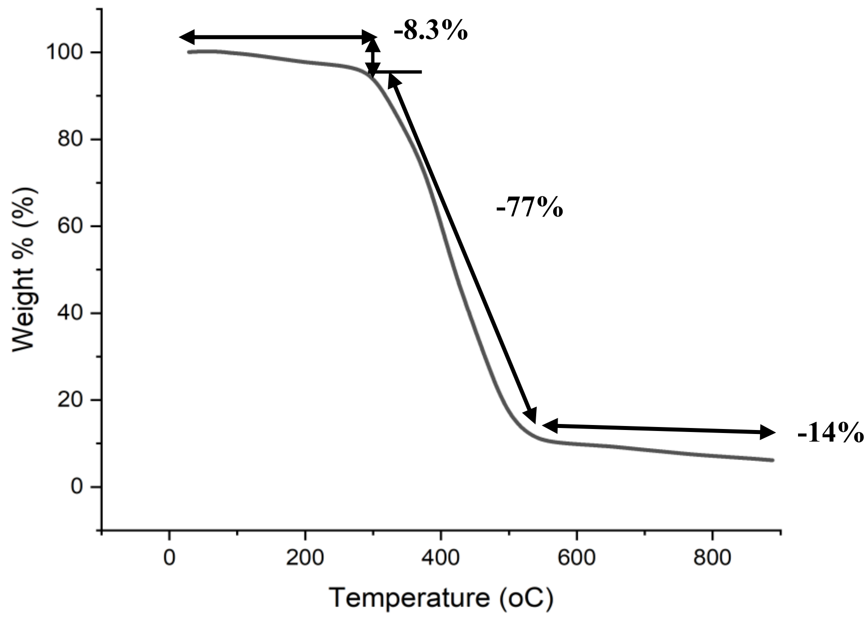

Figure 7: TGA spectra of the Zn-BPDC MOF sample

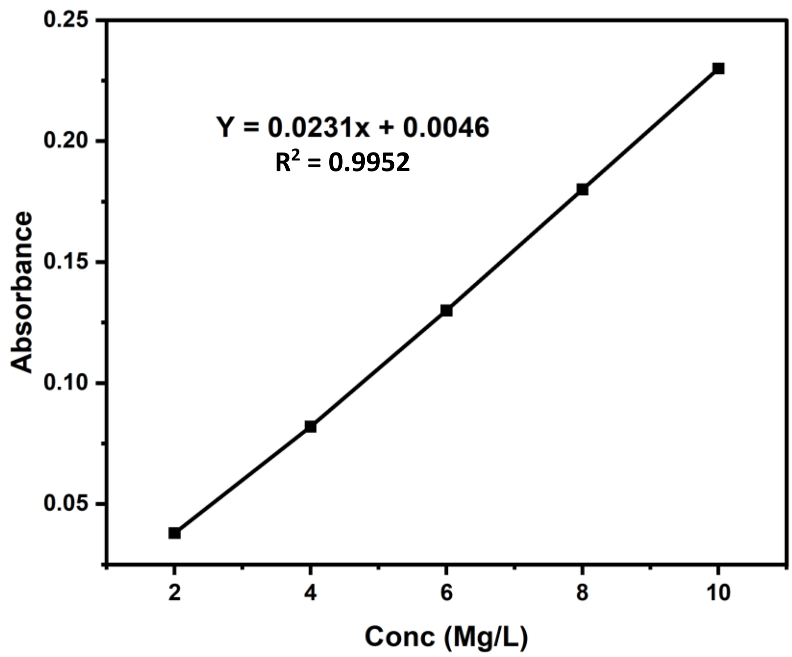

Figure 8: Calibration curve of Brilliant blue dye

Broad O–H stretching bands detected between 2500 and 2800 cm⁻¹ are indicative of hydrogen-bonded carboxylic acid groups (Smith, 2018). Additional bands missing from the free ligand in the Zn-BPDC MOF spectra indicate that the framework has assembled. Due to axial solvent coordination at Zn^{2+} centers, a broad absorption band near 3369 cm⁻¹ might be attributed to O–H stretching vibrations from coordinated or physically adsorbed solvent molecules, which are frequently seen in Zn-carboxylate MOFs (Zelenák *et al.,* 2008; Hadjiivanov *et al.,* 2020). The aromatic overtone/combination region contains a weak band at about 1938 cm⁻¹, which indicates stronger vibrational coupling and structural ordering of biphenyl units following framework formation (Hermans *et al.,* 2021; Liu *et al.,* 2022). In conclusion, the emergence of novel bands and modifications in carboxylate-related vibrations and intensities, which confirm coordination between BPDC ligands and Zn^{2+} ions, promote the development of Zn-BPDC MOF.

Table 2: Model Summary Statistics for Zn-MOF adsorption of Brilliant Blue

Source	Std. Dev.	R^2	Adjusted R^2	Predicted R^2	PRESS	
Linear	14.36	0.7645	0.7252	0.6494	7363.23	
2FI	16.51	0.7663	0.6365	0.3081	14530.50	
Quadratic	**1.02**	**0.9993**	**0.9986**	**0.9968**	**67.65**	**Suggested**
Cubic	1.26	0.9995	0.9979	0.9604	831.38	

Table 3: Experimental runs with the actual and predicted responses of adsorption of BB

	Factor 1	Factor 2	Factor 3	Factor 4	Response 1	
Run	A: Adsorbent Dosage (Grams)	B: Ionic Strength (Mol/L)	C: Time (Mins)	D: pH	Dyes Removal %	
					Actual	Predicted
1	0.3	0.17	30	7	29.25	29.26
2	0.1	0.17	75	7	18.33	18.88
3	0.1	0.085	30	7	18.47	18.00
4	0.3	0	75	2	91.52	91.26
5	0.5	0.17	75	7	40.86	40.55
6	0.5	0.085	30	7	42.12	41.63
7	0.3	0	30	7	31.07	31.34
8	0.5	0.085	120	7	41.84	41.44
9	0.5	0	75	7	44.64	43.60
10	0.3	0.085	75	7	27.01	27.90
11	0.1	0	75	7	18.61	18.44
12	0.3	0.085	30	2	89.84	90.09
13	0.3	0.085	75	7	29.39	27.90
14	0.3	0.085	75	7	27.71	27.90
15	0.3	0.085	120	2	91.38	90.46
16	0.5	0.085	75	2	97.82	99.09
17	0.3	0	75	12	22.53	22.38
18	0.3	0.17	120	7	28.97	30.06
19	0.3	0.085	75	7	27.15	27.90
20	0.3	0.17	75	2	91.10	90.37
21	0.3	0.085	120	12	21.55	20.82
22	0.5	0.085	75	12	34.71	35.68
23	0.3	0.085	75	7	28.27	27.90
24	0.3	0	120	7	29.25	30.59
25	0.3	0.17	75	12	21.27	20.66
26	0.3	0.085	30	12	20.71	21.14
27	0.1	0.085	120	7	18.61	18.23
28	0.1	0.085	75	12	6.30	6.38
29	0.1	0.085	75	2	81.16	81.55

Table 4: ANOVA data for the adsorption of Brilliant Blue onto Zn-MOF

Source	Sum of Squares	Degree of freedom	Mean Square	F-value	p-value	
Model	20986.29	14	1499.02	1449.94	< 0.0001	significant
A-dosage	1644.98	1	1644.98	1591.11	< 0.0001	
B-ionic strength	5.12	1	5.12	4.95	0.0430	
C-Time	0.0016	1	0.0016	0.0016	0.9689	
D-pH	14404.49	1	14404.49	13932.82	< 0.0001	
AB	3.06	1	3.06	2.96	0.1074	
AC	0.0441	1	0.0441	0.0426	0.8394	
AD	34.54	1	34.54	33.41	< 0.0001	
BC	0.5924	1	0.5924	0.5730	0.4616	
BD	0.1762	1	0.1762	0.1705	0.6859	
CD	0.1224	1	0.1224	0.1184	0.7359	
A^2	6.31	1	6.31	6.11	0.0269	
B^2	14.14	1	14.14	13.68	0.0024	
C^2	5.66	1	5.66	5.47	0.0346	
D^2	4654.58	1	4654.58	4502.17	< 0.0001	
Residual	14.47	14	1.03			
Lack of Fit	10.73	10	1.07	1.15	0.4866	not significant
Pure Error	3.74	4	0.9361			

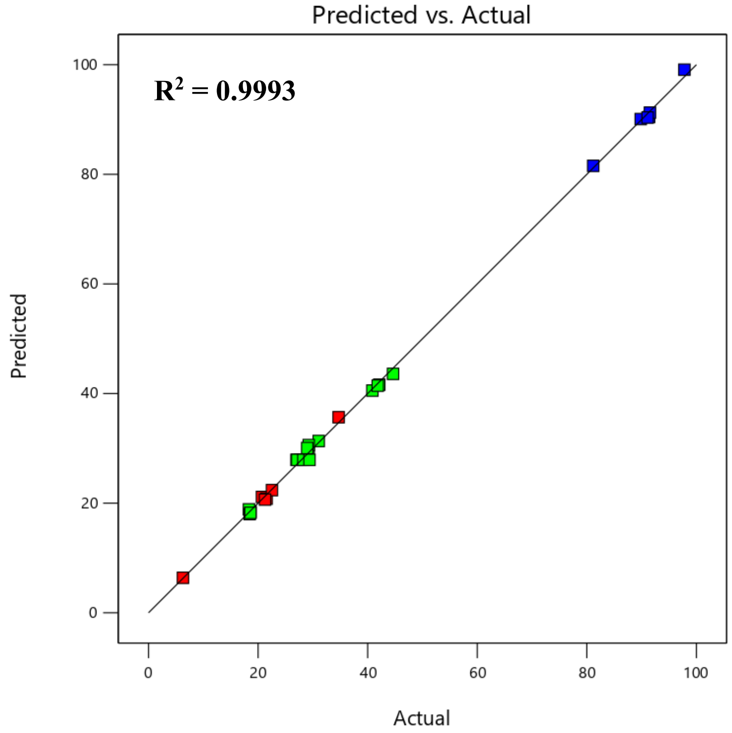

Figure 9: Fitting quality of the predicted and actual values

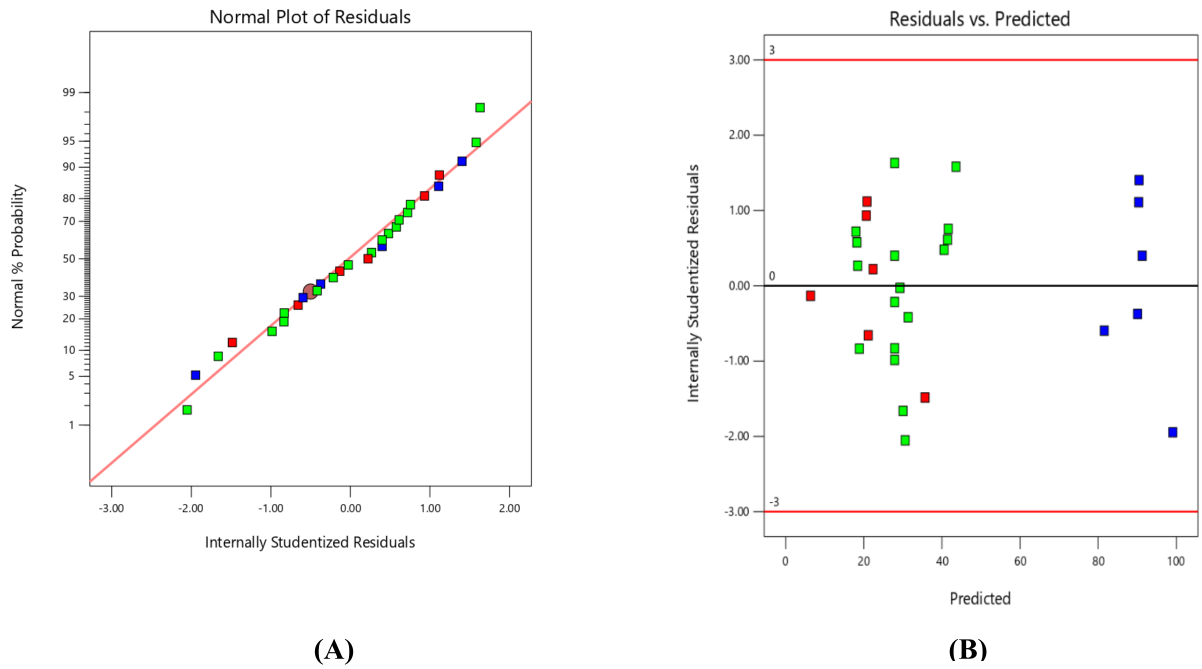

Figure 10 (A) Plot of the Internally studentized residual with normal probability, (B) plot of the predicted value against the internally studentized residuals of the Brilliant Blue dye adsorption by Zn-BPDC-MOF.

Figure 2 displays the Zn-BPDC MOF's EDXRF spectrum. X-ray fluorescence (XRF) spectroscopy was used to determine the elemental composition of the Zn–BPDC metal–organic framework (MOF) produced. Zinc is the only major metal atom found in the composite material, according to the approach; all other elements were present at negligible levels. Zn's integration into the framework is confirmed by the strong Zn Kα (8.6 keV) and Kβ (9.6 keV) emission lines in the spectrum. The high intensities of the Zn Kα and Kβ peaks confirm the successful incorporation of Zn^{2+} ions into the MOF framework. Therefore, the EDXRF analysis's result validates and confirms that zinc is the material's primary metallic component (Abid *et al.,* 2024; Pasandideh and Razmi, 2022)

In accordance with IUPAC recommendations for mesoporous and microporous solids, the BET surface area was calculated using the multi-point BET method in the linear portion of the BET plot, which corresponds to a relative pressure (P/P_0) range of 0.049–0.303 (Thommes *et al.,*2020). The material has a surface area of 221.022

m²/g, which is considered considerable, according to the BET study. Plotting PV (P0-P) versus relative pressures P/P0 made the estimation of key parameters, such as slope, intercept, and BET constant (C) possible, which were utilized to calculate the specific surface area (Figure 3A).

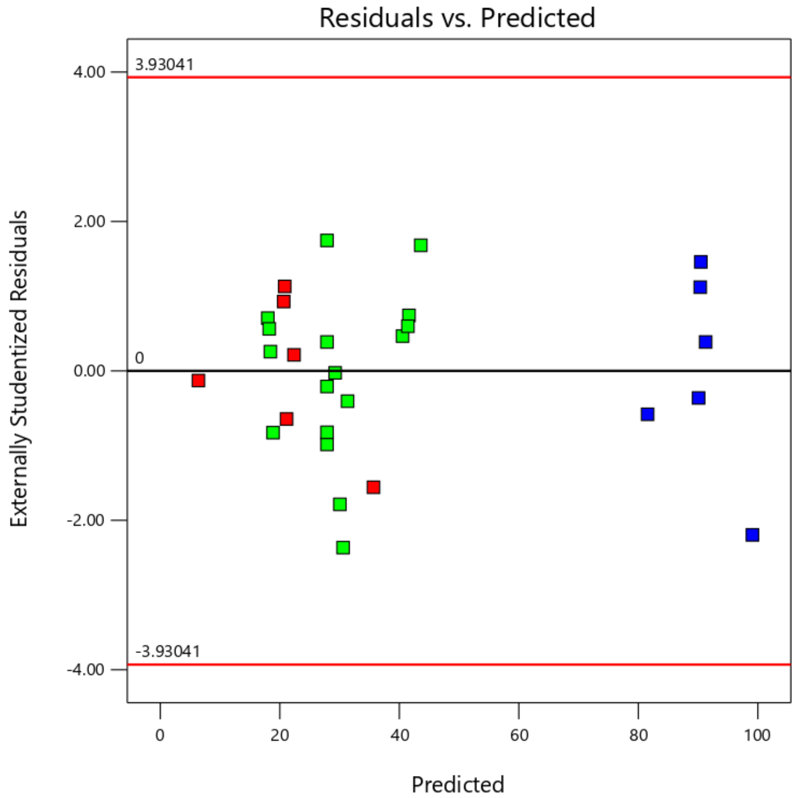

Figure 11: Plot of the predicted value against the externally studentized residuals of the Brilliant Blue dye adsorption by Zn-BPDC-MOF.

Figure 4 also displays the pore size distribution (PSD) plot. The linear regression analysis produced a slope of 12.518, an intercept of 3.239, a correlation coefficient (R^2) of 0.988, and a BET constant (C) of 4.865. The BET plot has a well-defined linear region. The Barrett–Joyner–Halenda (BJH) method was also used to assess the pore structure characteristics of the adsorbents. This technique provides information about pore size, pore volume, and mesopore distribution. The BJH data (Figure 3B) show an average pore diameter (BJH Dv(d)) of 2.118 nm and a pore volume of 0.134 cm³/g. With pore widths of about 2.12 nm, which fall within the IUPAC-defined mesopore range of 2–50 nm, this suggests that the material has mesoporosity. The material's accessible internal voids or cavities, a key feature of MOFs, are shown by the pore volume of 0.134 cm³/g, which increases the availability of active adsorption sites (Ren *et al.*,2013)

The surface of the synthesized BPDC-based MOF had a pH_{PZC} of 6 (Figure 5), indicating that it is positively charged at pH values below 6 and negatively charged at pH values above 6. This has direct implications for adsorption selectivity: cationic species are electrostatically favoured at pH > 6, while anionic species are favoured at pH < 6. The observed pH_{PZC} is in line with previously published BPDC-based frameworks, in which the metal node, synthetic and post-synthetic modifications, and the carboxylate linker environment frequently result in near-neutral pHPZC values (Ghaedi *et al.,* 2024; Dong *et al.,* 2019).

Figure 6 shows the XRD patterns of BPDC and the synthesized Zn-BPDC MOF. XRD analysis was used to assess the identity of the ligand, the materials' crystallinity, phase purity, and structural features. The Zn-BPDC MOF exhibited distinct diffraction peaks at 2θ = 16.92, 24.52, 25.23, and 26.78°, confirming its crystalline nature. The disappearance and shift of the characteristic BPDC peaks at 2θ = 13.01, 15.11, 28.89, 32.41, and 39.85° indicates successful coordination between the carboxylate groups of BPDC and Zn^{2+} ions, resulting in framework formation. A noticeable reduction in peak intensity was observed for the Zn-BPDC MOF compared to the pure ligand. This reduction does not indicate poor crystallinity but is attributed to a structural rearrangement following coordination of Zn(II) ions to BPDC ligands. Similar observations have been reported for Ni-BPDC MOFs synthesized via hydrothermal methods, in which reduced peak intensity was associated with framework formation and changes in crystallographic order rather than with a loss of crystallinity (Wang et al., 2019; Wang et al., 2020). The XRD pattern of the pure BPDC ligand is consistent with earlier reports (Zhang et al., 2021; Li et al., 2022). The presence of broad peaks may be attributed to partially crystalline or disordered MOF domains (Al-Zawahreh et al., 2024; Zhang et al., 2021). A similar reduction in peak intensity was also reported for a solvothermally synthesized Zn-BPDC MOF, in which partial loss of crystallinity was linked to activation and solvent retention within the porous framework (Guilherme et al., 2018).

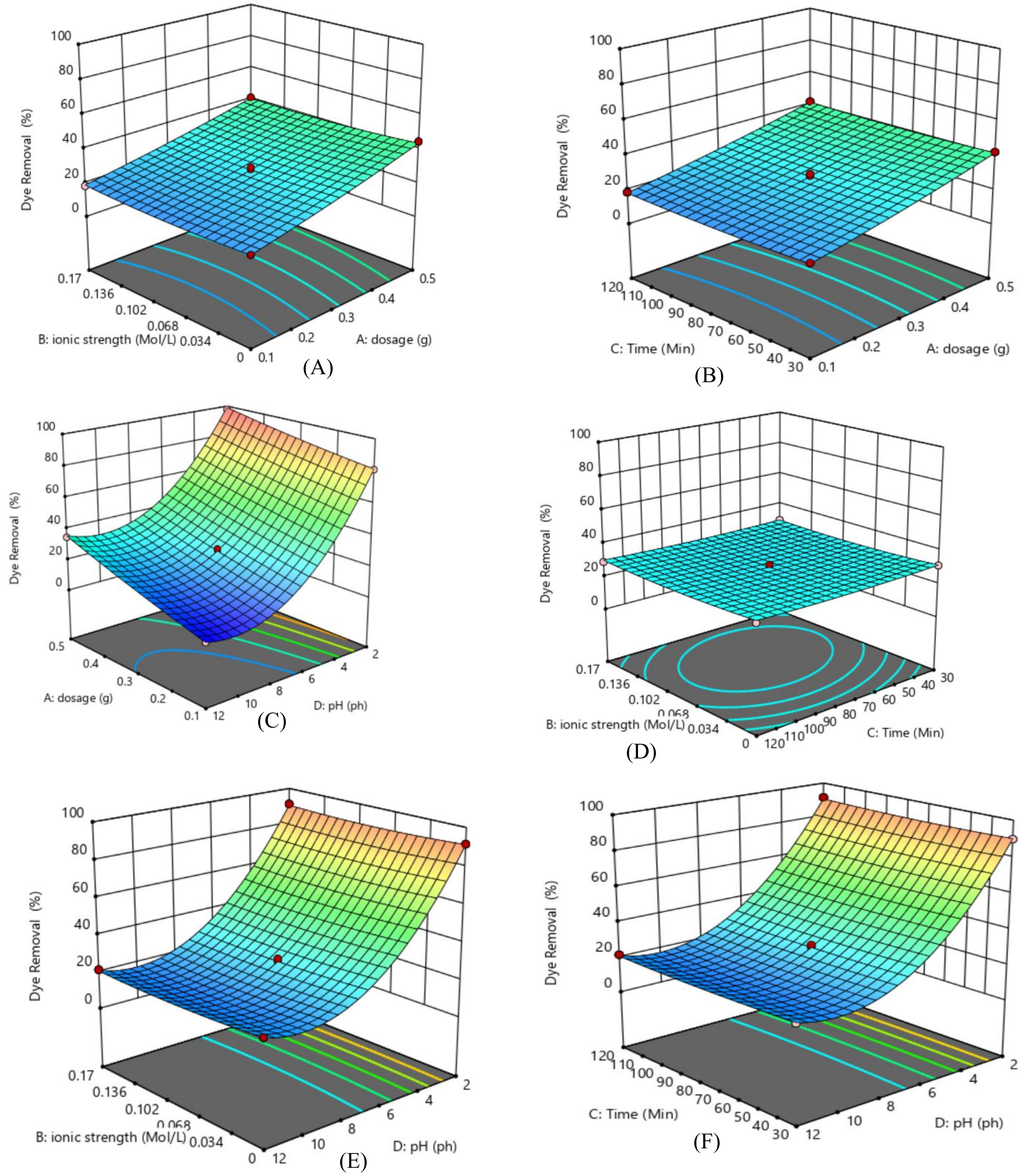

Figure 12 (A-F): 3D surface plots showing the effects of the four factors on Brilliant Blue dye adsorption by Zn-BPDC-MOF.

The thermal stability of the synthesized Zn-BPDC MOF was evaluated using a Perkin Elmer Thermal Analyzer over a temperature range of 30–950 °C at a heating rate of 10 °C min^{-1}. The TGA profile shown in Figure 7 exhibits three distinct weight-loss stages. The first stage, accounting for approximately 8.3% weight loss below 310 °C, is attributed to the removal of physically adsorbed water, residual solvent molecules, and traces of chlorine-containing species present in the material. The second and most significant weight-loss stage occurred between 311 and 512 °C, corresponding to about 77% mass loss and associated with the decomposition of the organic BPDC ligand and the carboxylate framework. A final weight loss of about 14% was observed above 520 °C, indicating the collapse of the MOF structure and the formation of ZnO as the thermally stable residual product. The stability of the material up to approximately 310 °C suggests that the synthesized Zn-BPDC MOF possesses adequate thermal resistance for potential adsorption and catalytic applications, which is consistent with previous reports on Zn-based MOFs (Zhang et al., 2021; Liu et al., 2022).

The calibration curve used for Brilliant Blue concentration determination (Figure 8) showed good linearity over the studied concentration range (2-10 Mg/L), with a regression coefficient (R^2) of 0.9952. The linear regression equation obtained was y = 0.0231x + 0.0046, where y is absorbance and x is dye concentration. The high R^2 value indicates a strong correlation between absorbance and concentration, confirming the reliability of the calibration model for accurate determination of residual dye concentrations during the adsorption experiments.

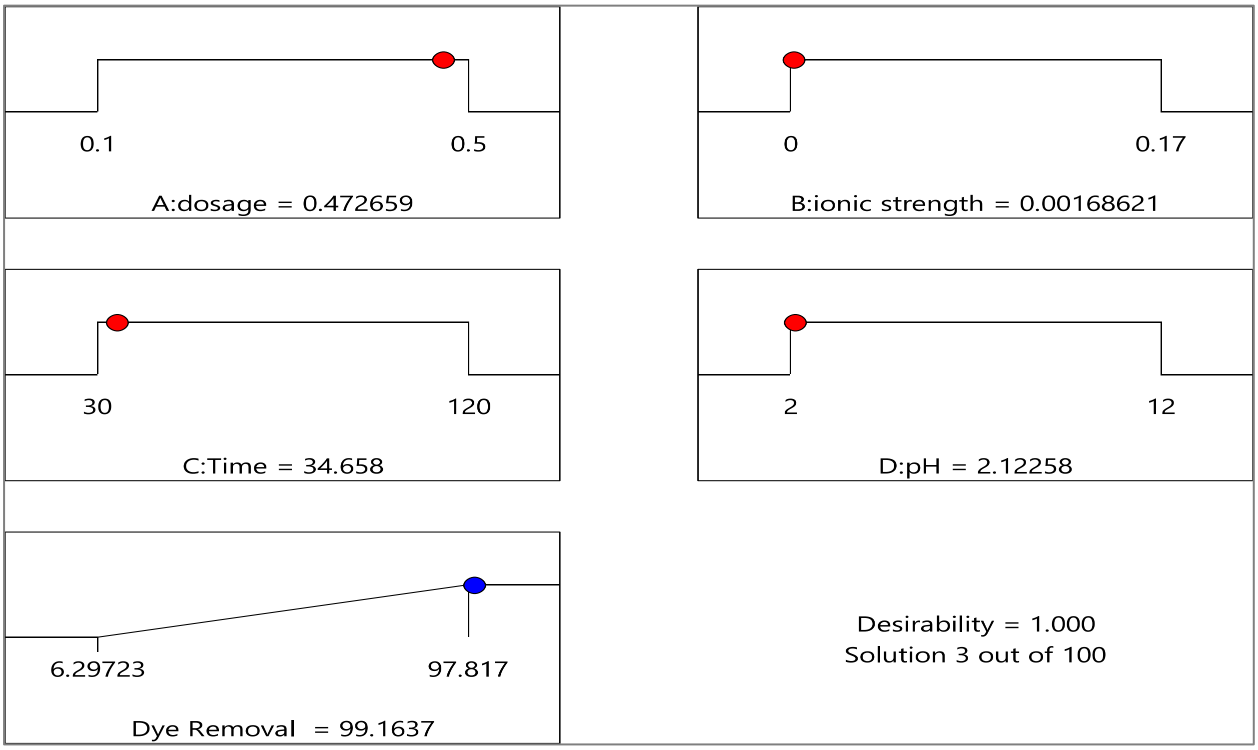

Figure 13: Optimization graph showing the best predicted values for optimum adsorption of Brilliant Blue dye by Zn-MOF

Table 5. RSM-Optimized condition of Brilliant blue adsorption on Zn-MOF

A (g)	B (Mol/L)	C (Min)	D (pH)	Dye Removal %		
				Actual	Predicted	qe (mg/g)
0.473	0.0017	34.66	2.12	98.33	99.16	6.22

3.3 Statistical Modelling and Optimization of BBD removal by BPDC-based Zn-MOF

3.3.1 Model summary statistics and adequacy

The linear 2FI, quadratic, and cubic equations of the Response Surface Methodology (RSM) were used to model the optimization parameters in this work, including pH, adsorbent dosage, time, and ionic strength. Table 2 makes clear that the quadratic model was recommended and selected since it has the lowest press, standard deviation, and difference between the adjusted R^2 and predicted R^2 values.

Table 3 presents the experimental design and the experimental and predicted percentage dye removal (% removal). The lowest BB adsorption was 6.30% at adsorbent dosage of 0.1g, ionic strength level of 0.085Mol/L, pH of 12, and 75 minutes, whereas the maximum removal percentage for brilliant blue adsorption was 97.82% at adsorbent dosage of 0.5g, ionic strength level of 0.085Mol/L, and pH level of 2 at 75 minutes. The regression equation for this experiment is shown as follows in terms of the actual values:

$$\text{Dye Removal (\%)} = 122.811 + 28.4192 \times A + -31.0746 \times B + -0.0685439 \times C + -22.7117 * D + -51.448 \times AB + -0.0116615 \times AC + 2.93871 \times AD + 0.100609 \times BC + -0.4939 \times BD + -0.000777436 \times CD + 24.6641 \times A^2 + 204.339 \times B^2 + 0.000461279 \times C^2 + 1.07151 \times D^2 \quad (4)$$

3.3.2 Regression Analysis and ANOVA

The analysis of variance (ANOVA) results shown in Table 4 were used to analyze the model. The statistical significance of the model was assessed using the Fisher test; a higher Fisher's F value is considered to suggest a more suitable and significant model (Sheikhi *et al.,* 2020). The model was found to be relevant and suitable for design monitoring. The tiny p-value ($p < 0.05$) of the quadratic model indicates its statistical significance and its ability to predict BBD dye removal with high accuracy and precision (Kothari *et al.,* 2022; Gadekar and Ahammed, 2019). It is important to remember that if a term's p-value is more than 0.05, it is considered statistically insignificant (Nguyen *et al.,* 2022). The model was found to be significant and suitable for design monitoring. The quadratic model's tiny p-value ($p < 0.05$) indicates its statistical significance and great accuracy and precision in predicting BBD dye elimination (Ahmadi *et al.,* 2018; Gadekar and Ahammed, 2019). A F value of 1.15 means that the lack of fit is not statistically significant in comparison to pure error. This magnitude of lack of fit F-value has a 48.66% probability of being due to random variation. A lack of fit that is not statistically significant is a good thing. The model fits the experimental data well and the independent process variables significantly affect the response if the p-value for lack of fit is more than 0.05 (Bezerra *et al.,* 2008)

3.3.3 Adequacy of the model

Table 3 showed the percentage of actual and expected (predicted) values for BBD elimination data. The primary objective of using regression models is to further ascertain the model's ability to predict the response variable. As seen in Figure 9, plotting the predicted value of BBD adsorption against the actual value from data results in an R^2 value of 0.9993, which validates the models' accuracy and may be used in the experiment (Yousefi *et al.,* 2022)

3.3.4 Residuals' Normal Probability Plot (NPP)

The normal probability plot (NPP) of the residuals is a crucial statistical tool for assessing the appropriateness of the model. Figure 10A displays the NPP of the residuals for the adsorption of brilliant blue dye. The data analysis shows that the residuals are distributed along the normal distribution's diagonal. This implies that the model is suitable. Figure 10B displays a graph of residual versus predicted brilliant blue dye percent removal data. The points in this graph, which cluster around the diagonal line, demonstrate how well the model fits the data. The plot of the predicted value against the externally studentized residuals is also presented in Figure 11 (Ahmad *et al.,* 2021)

3.3.5 3D Surface Plots

In order to assess response value variation and identify the ideal conditions of the variables that will result in the highest present dye removal for BBD in aqueous solutions, three-dimensional (3D) surface plots were analyzed and used to illustrate the influence of the process parameters (independent variables) and the dependent variable (percent dye uptake). The 3D graphs in Figure 12 illustrate the effects of the initial pH of the dye solution, the adsorbent dose, and other factors. These figures clearly show that the pH solutions and the adsorbent dosage significantly influenced the proportion of dyes removed in each experimental run.

As there are more sorption sites for the adsorbent in the system, the percentage of BBD elimination increases with higher adsorbent dosage levels (Shah *et al.,* 2013). Similarly, the outcome of the adsorbent's point of zero charge (Figure 5) can be directly linked to the effect of pH on the percentage of BBD removal. The adsorbent was found to have a pH_{ZPC} of 6. Above this pH, the adsorbent's surface has a high net negative charge density, which explains its poor affinity for the negatively charged dye (at pH 7 and 12). Below pH 6, on the other hand, its surface is dominated by positive charge, which explains its high affinity for the negatively charged dye in this study (at pH of 2). The optimum pH of 2.12 obtained from the RSM model can be attributed to the positively charged surface of the Zn–BPDC MOF at pH values below its pHPZC (6), which enhances electrostatic attraction between the adsorbent surface and the anionic Brilliant Blue dye molecules, resulting in improved adsorption. The 3D figure and its P-Value (Table 4) also show that the time and ionic strength factors had no significant effects.

3.3.6 Desirability Function (DF) and Process Optimization

In chemistry, process optimization is crucial for reducing expenses, time, and energy in multi-response approaches (Singh *et al.,* 2022). To determine the best-predicted probability, the desirability function was applied to the highest response (per cent dye removal). The values of the desirability function vary from undesired (0) to desirable (1) (Kumari *et al.,* 2023). Figure 13's optimization chart shows the optimal percentage removal of BBD and the best-predicted spots for the intended purpose. According to this desirability function, the predicted conditions for the highest percentage of BBD removal were 0.473 grams of adsorbent, pH 2.12, ionic strength 0.0017 mol/L, and 34.66 minutes. This yielded a predicted dye removal percentage of 99.16% compared to the observed experimental removal percentage of 98.33% (Table 5).

CONCLUSION

A solvent-free mechanochemical synthetic route was employed to prepare a Zn-BPDC MOF adsorbent for the removal of Brilliant Blue dye (BBD) from aqueous synthetic wastewater. FTIR, EDXRF, BET, XRD, TGA, and pHPZC characterization analyses confirmed the incorporation of zinc into the ligand framework and its thermal stability. Using 29 experimental runs generated by the Box–Behnken design of response surface methodology, the effects of adsorbent dosage, ionic strength, contact time, and pH on the adsorption process were evaluated. The optimum conditions were determined to be an adsorbent dosage of 0.473 g, ionic strength of 0.0017 mol L^{-1}, contact time of 34.66 min, and pH of 2.12, resulting in a maximum BBD removal efficiency of 98.33%. The study demonstrated the effectiveness of response surface methodology in optimizing the adsorption process and identifying the conditions required for maximum dye removal.

However, it -should be noted that the adsorption experiments were conducted using synthetic dye solutions under controlled laboratory conditions, which may not fully reflect the complexity of real industrial effluents. In addition, regeneration, reusability, and metal leaching studies were not performed, and the long-term stability of the synthesized Zn-BPDC MOF remains to be established in future studies. Furthermore, the optimum adsorption occurred at a strongly acidic pH of 2.12, which may increase chemical consumption and operational costs in practical wastewater treatment applications. In future studies, the researchers will focus on determining adsorption capacity from isotherm studies using the optimum conditions established by the developed model in this study, on regeneration and reusability assessments, and on validation using real wastewater.

DECLARATION OF COMPETING INTEREST

The authors declare that they have no known competing financial interests or personal relationships that could have appeared to influence the work reported in this paper.

REFERENCES

Abid, H. R., Khan, A., Amin, M., & Alajerami, Y. S. (2024). Physicochemical characterization of metal-organic frameworks: The role of XRF and PIXE in structural and compositional assessment. *Journal of Materials Chemistry A*, 12 (14), 2674-2690. [Crossref]

Adamu, K. S., & Salisu, I. (2024). Optimization of polyhydroxybutyrate production by *Bacillus* species isolated from dump site soil using multiple linear regression analysis. *UMYU Scientifica*, 3(4), 355-368. [Crossref]

Adeleke, A. J., Adeyemo, O. M., Mashigira, A. S., & Antia, U. E. (2025). Valorization of Goruba (*Hyphaene thebaica* L) fruit waste for optimized prebiotic xylooligosaccharides production via *Aspergillus flavus* xylanase. *UMYU Scientifica*, 4(2), 334-342. [Crossref]

Ahmad, A. L., Wong, S. S., Teng, T. T., & Zuhairi, A. (2021). Optimization of coagulation-flocculation process for dye removal using response surface methodology and model diagnostic analysis. *Journal of Water Process Engineering*, 40, 101930. [Crossref]

Ahmadi, S., Mohammadi, L., Igwegbe, C. A., Rahdar, S., & Banach, A. M. (2018). Application of response surface methodology in the degradation of Reactive Blue 19 using H_2O_2/MgO nanoparticles advanced oxidation process. *International Journal of Industrial Chemistry*, 9(3), 241-253. [Crossref]

Akeremale, O. K. (2022). Metal-organic frameworks (MOFs) as adsorbents for purification of dye-contaminated wastewater: A review. *Journal of Chemical Reviews*, 4(1), 1-14. [Crossref]

Akeremale, O. K., Aworetan, J., & Aworetan, O. (2025). Design techniques and applications of ionic liquids incorporated metal organic frameworks (IL/MOFs). *American Journal of Physical Chemistry*, 14(2), 33-50. [Crossref]

Akeremale, O. K., Ore, O. T., Bayode, A. A., Badamasi, H., Olusola, J. A., & Durodola, S. S. (2023). Synthesis, characterization and activation of metal organic frameworks for the removal of emerging organic contaminants through adsorption-oriented process: A review. *Results in Chemistry*, 5, 100866. [Crossref]

Akeremale, O. K., & Olaseni, S. E. (2019). Comparative studies on the adsorption of rhodamine B and malachite green from simulated wastewater onto bentonite clay. *ChemSearch Journal*, 10(2), 30-40.

Alam, M. M., Ahmad, M., & Hossain, M. A. (2024). Recent advances in the removal of triphenylmethane dyes from wastewater using adsorptive materials: Mechanisms and environmental perspectives. *Journal of Water Process Engineering*, 59, 105053. [Crossref]

Ali, I., Peng, C., Naz, I., Khan, Z. H., & Shah, M. R. (2022). Low-cost adsorbents for wastewater treatment: Recent developments, challenges, and future perspectives. *Environmental Research*, 212, 113261.

Al-Zawahreh, K., Barral, M. T., & Paradelo, R. (2024). Overview of factors to take into account when selecting high-grade dye adsorbents. *Environmental Technology Reviews*, 13(1), 597-613. [Crossref]

Balistrieri, L. S., & Murray, J. W. (1981). The surface chemistry of goethite (α-FeOOH) in major ion seawater. *American Journal of Science*, 281, 788-806. [Crossref]

Bezerra, M. A., Santelli, R. E., Oliveira, E. P., Villar, L. S., & Escaleira, L. A. (2008). Response surface methodology (RSM) as a tool for optimization in analytical chemistry. *Talanta*, 76(5), 965-977. [Crossref]

Chen, W.-H., Uribe, M. C., Kwon, E. E., Lin, K.-Y. A., Park, Y.-K., Ding, L., & Saw, L. H. (2022). A comprehensive review of thermoelectric generation optimization by statistical approach: Taguchi method, analysis of variance (ANOVA), and response surface methodology (RSM). *Renewable and Sustainable Energy Reviews*, 169, 112917. [Crossref]

Dong, X., Lin, Y., Ma, Y., & Zhao, L. (2019). Ce-doped UiO-67 nanocrystals with improved adsorption property for removal of organic dyes. *RSC Advances*, 9, 27674-27683. [Crossref]

Duan, J., Jin, W., & Kitagawa, S. (2023). Metal-organic frameworks for advanced applications: From design to functional materials. *Chemical Society Reviews*, 52(2), 565-637.

Flórez, E., Jimenez-Orozco, C., & Acelas, N. (2024). Unravelling the influence of surface functional groups and surface charge on heavy metal adsorption onto carbonaceous materials: An in-depth DFT study. *Materials Today Communications*, 39, 108647. [Crossref]

Gadekar, M. R., & Ahammed, M. M. (2019). Modelling dye removal by adsorption onto water treatment residuals using combined response surface methodology-artificial neural network approach. *Journal of Environmental Management*, 231, 241-248. [Crossref]

Ghaedi, S., Rajabi, H., Mosleh, M. H., Babakhani, P., & Sedighi, M. (2024). UiO-67 metal-organic framework loaded on hardwood biochar for sustainable management of environmental boron contamination. *Journal of Environmental Chemical Engineering*, 12(6), 114511. [Crossref]

Ghosh, A., & Gupta, A. (2013). Removal of azo dyes from water by adsorption onto metal oxide nanoparticles. *Environmental Science & Technology*, 47(4), 1685-1692.

Głowniak, S., Szczęśniak, B., Choma, J., & Jaroniec, M. (2024). Mechanochemical synthesis of MOF-303 and its CO_2 adsorption at ambient conditions. *Molecules*, 29(11), 2698. [Crossref]

Guilherme, N. L., Renata, C. A., Marina, P. A., Leila, A. C., Isabel, C. d-S., Fernando, R. P., Regina, & Célia, G. F. (2018). Zn-based porous coordination solid as diclofenac sodium carrier. *Journal of Solid State Chemistry*, 260, 67-72. [Crossref]

Habibu, S., Ladan, M., Safana, A. A., Dandalma, Z. A., Saleh, I., & Abdullahi, S. R. (2023). Optimization of methylene blue adsorption onto activated carbon derived from pineapple peel waste using response surface methodology. *UMYU Scientifica*, 2(4), 45-55. [Crossref]

Hadjiivanov, K. I., Mihaylov, M. Y., Chakarova, K. K., & Ivanova, E. Z. (2020). Power of infrared and Raman spectroscopies to characterize metal-organic frameworks and related materials. *Chemical Reviews*, 120(16), 12389-12459. [Crossref]

Hasanzadeh, R., Mojaver, M., Azdast, T., & Park, C. B. (2021). Polyethylene waste gasification syngas analysis and multi-objective optimization using central composite design for simultaneous minimization of required heat and maximization of exergy efficiency. *Energy Conversion and Management*, 247, 114713. [Crossref]

Hermans, J. J., Smeets, P. J. M., & Reek, J. N. H. (2021). Nature of zinc carboxylate coordination in hybrid frameworks: An FTIR and XPS study. *Inorganic Chemistry*, 60(4), 2151-2162. [Crossref]

Hosseinpour, V., Kazemeini, M., & Mohammadrezaee, A. (2011). Optimization of Ru-promoted Ir-catalyzed methanol carbonylation utilizing response surface methodology. *Applied Catalysis A: General*, 394, 166-175. [Crossref]

Ibrahim, U. B., Yusuf, I., Saleh, A., Fardami, A. Y., Nataala, M. K., Yahaya, H. I., Jodi, A. M., Sanusi, Z. M., Yahaya, S., & Kawo, A. H. (2023). Biomass assessment and optimization of *Alcaligenes faecalis* isolated from some Nigerian mining sites for heavy metal uptake using response surface methodology model. *UMYU Scientifica*, 2(3), 128-141. [Crossref]

Imran, M., Crowley, D. E., Khalid, A., Hussain, S., Mumtaz, M. W., & Arshad, M. (2021). Microbial biotechnology for decolorization of textile wastewaters. *Reviews in Environmental Science and Bio/Technology*, 20, 737-764. [Crossref]

Jang, H. M., Kan, E., & Lee, S. H. (2020). Insights to perfluorooctanoic acid adsorption micro-mechanism over Fe-based metal organic frameworks: Combining computational calculation with response surface methodology. *Journal of Hazardous Materials*, 395, 122686. [Crossref]

Jawad, A. H., Abdulhameed, A. S., & Mastuli, M. S. (2023). Adsorption of synthetic dyes from aqueous solution by low-cost adsorbents: A review of recent developments and adsorption mechanisms. *Journal of Water Process Engineering*, 53, 103624.

Julien, A. P., Užarević, K., Katsenis, D. A., Kimber, S. A. J., Wang, C. T., Farha, K. O., Zhang, Y., Casaban, J., Germann, L., Etter, M., Dinnebier, E. R., James, L. S., Halasz, I., & Friščić, T. (2016). In situ monitoring and mechanism of the mechanochemical formation of a microporous MOF-74 framework. *Journal of the American Chemical Society*, 138(9), 2929-2932. [Crossref]

Kalia, S., Samuchiwal, S., Dhaka, V., & Malik, A. (2023). Development and optimization of the dye removal process by *Trichoderma reesei* using starch effluent as a growth supplement. *AQUA - Water Infrastructure, Ecosystems and Society*, 72(3), 395-410. [Crossref]

Katheresan, V., Kansedo, J., & Lau, S. Y. (2023). Efficiency of various recent wastewater dye removal methods: A review. *Journal of Environmental Chemical Engineering*, 11(1), 109012.

Khan, A. K., Shah, A., & Nisar, J. (2024). Electrochemical detection and removal of brilliant blue dye via photocatalytic degradation and adsorption using phyto-synthesized nanoparticles. *RSC Advances*, 14, 1854-1865. [Crossref]

Khan, A., Naeem, A., & Mahmood, T. (2020). Thermodynamic study of adsorption of methyl orange and Congo red from aqueous solutions by PVP-functionalized ZnO. *Russian Journal of Physical Chemistry A*, 94, 1581-1586. [Crossref]

Kothari, M. S., Vegad, K. G., Shah, K. A., & Hassan, A. A. (2022). An artificial neural network combined with response surface methodology approach for modelling and optimization of electro-coagulation for dye removal. *Heliyon*, 8(1), e08749. [Crossref]

Kumari, S., Verma, A., Sharma, P., Agarwal, S., Rajput, V. D., Minkina, T., Rajput, P., Singh, S. P., & Garg, M. C. (2023). Introducing machine learning model to response surface methodology for biosorption of methylene blue dye using *Triticum aestivum* biomass. *Scientific Reports*, 13, 8574. [Crossref]

Lamidi, S., Olaleye, N. O., Bankole, Y. O., Obalola, A., Aribike, E., & Adigun, I. (2022). Applications of response surface methodology (RSM) in product design, development, and process optimization. *IntechOpen*. [Crossref]

Li, S., Wu, H., Jin, M., Lu, S., & Zhang, Y. (2022). 4,4'-Biphenyldicarboxylic acid-based Zn-MOFs: Structure, porosity, and electrochemical behavior. *Nanomaterials*, 12(12), 2062. [Crossref]

Liao, C. H., et al. (2017). Removal of azo dyes using nanoparticles of metal oxides: A review. *Journal of Environmental Management*, 201, 208-222.

Liu, X., Zhang, Y., & Chen, Q. (2022). Infrared and structural characterization of Zn-BPDC coordination polymers. *Journal of Molecular Structure*, 1256, 132574. [Crossref]

Mahmood, T., Ugur, S., Imer, Y., & D. (2024). Determination of brilliant blue FCF in food samples using hydrophilic deep eutectic solvent-assisted dispersive microextraction. *Food Chemistry*, 436, 137710. [Crossref]

Montgomery, D. C. (2020). *Design and analysis of experiments* (10th ed.). John Wiley & Sons.

Nandiyanto, A. B. D., Ragadhita, R., & Fiandini, M. (2022). Interpretation of Fourier transform infrared spectra (FTIR): A practical approach in the polymer/plastic thermal decomposition. *Indonesian Journal of Science and Technology*, 8(1), 113-126. [Crossref]

Nguyen, T. T. T., Hoang, D. Q., & Nguyen, D. T. C. (2022). Adsorptive optimization of crystal violet dye using central composite rotatable design and response surface methodology: Statistical analysis, kinetic and isotherm studies. *International Journal of Molecular Sciences*, 23(19), 11827. [Crossref]

Nidheesh, P. V., Zhou, M., & Oturan, M. A. (2023). An overview on the removal of synthetic dyes from water by advanced oxidation processes, adsorption, coagulation/flocculation, and biological methods. *Chemosphere*, 326, 138353.

Olaseni, S. E., Akeremale, O. K., & Aboluwoye, C. O. (2019). Removal of single and binary basic dyes from synthetic wastewater using bentonite clay adsorbent. *American Journal of Polymer Science and Technology*, 5(1), 16-28. [Crossref]

Pasandideh, Y., & Razmi, H. (2022). Introduction of a Zn-based metal-organic framework@biomass porous activated carbon as a high-sensitive coating for a stainless steel SPME fiber: Application to the simultaneous analysis of nonsteroidal anti-inflammatory drugs. *BMC Chemistry*, 16, 25. [Crossref]

Pavan, F. A., et al. (2014). Removal of azo dyes by polystyrene-based adsorbents. *Journal of Hazardous Materials*, 277, 32-41.

Qiu, S., & Zhu, G. (2022). Molecular engineering of metal-organic frameworks for adsorption and separation applications. *Coordination Chemistry Reviews*, 451, 214262.

Ren, T.-Z., Zhu, X.-H., Ma, T.-Y., & Yuan, Z.-Y. (2013). Adsorption of methylene blue from aqueous solution by periodic mesoporous titanium phosphonate materials. *Adsorption Science & Technology*, 31(6), 535-548. [Crossref]

Sari, A., & Tuzen, M. (2008). A comparative study of the adsorption of azo dyes from aqueous solution by various adsorbents. *Journal of Hazardous Materials*, 157(1), 189-195.

Selvam, P. P., Preethi, S., Basakaralingam, P., Thinakaran, N., Sivasamy, A., & Sivanesan, S. (2008). Removal of rhodamine B from aqueous solution by adsorption onto sodium montmorillonite. *Journal of Hazardous Materials*, 155(1-2), 39-44. [Crossref]

Shah, J., Rasul Jan, M., Haq, A., & Khan, Y. (2013). Removal of rhodamine B from aqueous solutions and wastewater by walnut shells: Kinetics, equilibrium and thermodynamics studies. *Frontiers of Chemical Science and Engineering*, 7(4), 428-436. [Crossref]

Sheikhi Alman-Abad, Z., Pirkharrati, H., Asadzadeh, F., & Maleki-Kakelar, M. (2020). Application of response surface methodology for optimization of zinc elimination from a polluted soil using tartaric acid. *Transactions of the Institute of Metal Finishing*, 98(3), 123-131. [Crossref]

Singh, S., Kumar, R., & Gupta, V. K. (2022). Process optimization and multi-response surface methodology approach in chemical and environmental engineering applications: A review. *Chemical Engineering Journal Advances*, 11, 100313. [Crossref]

Smith, B. C. (2016). Distinguishing structural isomers: Mono- and disubstituted benzene rings. *Spectroscopy*, 31(5), 36-39.

Smith, B. C. (2018). Infrared spectral interpretation: A practical guide. *Spectroscopy*, 33(1), 14-21.

Thommes, M., Kaneko, K., Neimark, V. A., Olivier, P. J., Rodriguez-Reinoso, F., Rouquerol, J., & Sing, K. S. W. (2020). Physisorption of gases, with special reference to the evaluation of surface area and pore size distribution (IUPAC Technical Report). *Pure and Applied Chemistry*, 92(3), 601-638. [Crossref]

Tkaczyk, A., Mitrowska, K., & Posyniak, A. (2020). Synthetic organic dyes as contaminants of the aquatic environment and their implications for ecosystems: A review. *Science of the Total Environment*, 717, 137222. [Crossref]

Vinothkumar, V., Chandra Sekhar, Y., Chen, S.-M., Manjula, N., & Kim, T. H. (2025). A sensitive and selective sensor based on orthorhombic copper molybdate decorated on reduced graphene oxide for the detection of promethazine hydrochloride. *Sensors*, 25(11), 3569. [Crossref]

Wang, X., Li, Q., Yang, N., He, F., Chu, J., Gong, M., Wu, B., Zhang, R., & Xiong, S. (2019). Hydrothermal synthesis of NiCo-based bimetal-organic frameworks as electrode materials for supercapacitors. *Journal of Solid State Chemistry*, 270, 370-378. [Crossref]

Wang, X., Yang, N., Li, Q., He, F., Yang, Y., Cong, S., Li, K., Xiong, S., & Zhou, A. (2020). Hydrothermal synthesis of humate-layer-based bimetal-organic framework composites as high rate-capability and energy-density electrode materials for supercapacitors. *ChemistrySelect*, 5, 2794-2804. [Crossref]

Xing, Y., Liu, D., & Zhang, L. P. (2010). Enhanced adsorption of methylene blue by EDTA-modified sugarcane bagasse and photocatalytic regeneration of the adsorbent. *Desalination*, 259, 187-191. [Crossref]

Yadav, V., Ali, J., & Garg, M. C. (2021). Biosorption of methylene blue dye from textile-industry wastewater onto sugarcane bagasse: Response surface modeling, isotherms, kinetic and thermodynamic modeling. *Journal of Hazardous, Toxic, and Radioactive Waste*, 25(4), 04020067. [Crossref]

Yousefi, M., Mahvi, A. H., & Azari, A. (2022). Modeling and optimization of dye removal using response surface methodology: Validation through predicted vs experimental values and regression analysis. *Environmental Science and Pollution Research*, 29, 56784-56798. [Crossref]

Yu, W., Luo, M., Yang, Y., Wu, H., Huang, W., Zeng, K., & Luo, F. (2019). Metal-organic framework (MOF) showing both ultrahigh As(V) and As(III) removal from aqueous solution. *Journal of Solid State Chemistry*, 269, 264-270. [Crossref]

Zaid, H., Al-sharify, Z.-T., Hamzah, M.-H., & Rushdi, S. (2022). Optimization of different chemical processes using response surface methodology - A review. *Journal of Engineering and Sustainable Development*, 26(6). [Crossref]

Zelenák, V., Gyepesová, D., & Orendáčová, A. (2008). Infrared spectroscopy study of zinc(II) carboxylates: Correlation of spectral features with structural modes. *Vibrational Spectroscopy*, 48(1), 63-68. [Crossref]

Zhang, X., Chen, C., & Wang, J. (2021). Morphological evaluation and adsorption performance of ZIF-8 for organic dyes. *Journal of Porous Materials*, 28(5), 1573-1582. [Crossref]